Anais da Academia Brasileira de Ciências (2019) 91(4): e20180817
(Annals of the Brazilian Academy of Sciences)
Printed version ISSN 0001-3765 / Online version ISSN 1678-2690
http://dx.doi.org/10.1590/0001-3765201920180817
www.scielo.br/aabc | www.fb.com/aabcjournal

Dendritic Gold Nanoparticles Towards Transparent and Electroactive Electrodes

RODRIGO M. IOST[1,3], MARCCUS V.A. MARTINS[2,3] and FRANK N. CRESPILHO[1]

[1]São Carlos Institute of Chemistry, University of São Paulo, Av. Trabalhador São-carlense, 400, 13560-970 São Carlos, SP, Brazil
[2]Federal Institute of Goiás, Av. Universitária Vereador Vagner da Silva Ferreira, Quadra 1,
Lote 1-A, s/n, Parque Itatiaia, 74968-755 Aparecida de Goiânia, GO, Brazil
[3]Centro de Ciências Naturais e Humanas, Universidade Federal do ABC, Avenida
dos Estados, 5001, 09210-580 Santo André, SP, Brazil

Manuscript received on August 6, 2018; accepted for publication on June 17, 2019

How to cite: IOST RM, MARTINS MVA AND CRESPILHO FN. 2019. Dendritic Gold Nanoparticles Towards Transparent and Electroactive Electrodes. An Acad Bras Cienc 91: e20180817. DOI 10.1590/0001-3765201920180817.

Abstract: The combination of UV-visible absorption and electrochemical experiments (spectroelectrochemistry) enables to obtain highly specific spectroscopic information (in situ and operando) from modified surfaces. However, such application can be limited by the self-absorbance, for example, when metallic nanoparticles are present on modified surfaces. Indium-tin oxide onto glass (ITO) is a typical electrode commonly used for spectroelectrochemistry; ITO is an oxide-based semiconductor, and in numerous applications it is necessary to promote the modification of the electrode surface without significant loss of transparency. Here, we report a simple strategy to obtain ITO electrodes modified with self-assembled polyelectrolytes and active dendritic gold nanoparticles (AuNPs), a combination of soft and metallic materials that results in electrodes with significant optical transparency. Self-assembled poly(sodium styrene sulfonate) and polyamidoamine dendrimer (PSS/PAMAN bilayer) were applied successfully as efficient platform for monodisperse dendritic AuNPs electrodeposition, and the electrode containing those materials shows substantial optical transmittance from 400nm to 800nm. The combination of transparency and the presence of AuNPs homogeneously dispersed start to be a practical approach to develop metal-based electrodes for spectroelectrochemistry.

Key words: indium tin oxide, gold nanoparticles, thin film, electrodeposition.

INTRODUCTION

Indium tin oxide (ITO) is a heavily-doped n-type semiconductor and one of the most widely used transparent conducting oxides. Due to its large band gap (~ 4 eV), ITO is mostly transparent in the visible spectrum and the coating of ITO on glass substrate shows several applications in electronic devices, with achievement of the products based on conducting transparent electrodes for electronic industry (Madaria et al. 2010). Others optically transparent and electrically conductive solid substrates have also been developed, such as glassy-modified with organic materials, e.g., polyaniline (Sapp et al. 1998), graphene sheets (Chen et al. 2009), carbon nanotubes networks (Li et al. 2006) and poly(3,4-ethylenedioxythiophene (Yan et al. 2005). In electrochemistry, the use of ITO electrodes is not only important because of the conductivity but aalso because of the properties

Correspondence to: Frank Nelson Crespilho
E-mail: frankcrespilho@iqsc.usp.br
ORCID: https://orcid.org/0000-0003-4830-652X

of transparency. Also, ITO is very important for applications in spectroelectrochemistry, organic electronics (Domingues et al. 2011), electrochromism (Zhao et al. 2009), solar cells (Ito et al. 2009) and photovoltaic devices (Armstrong et al. 2003).

One interesting feature is to modify ITO surface with functional nanostructured materials for practical applications (Richardson et. al 2015). At the same time it is important to obtain ITO-modified electrodes by a simple manner and without damage of the electrical and transparency properties of the electrode. Among the various materials used as modifiers of the ITO electrodes, the use of gold nanoparticles (AuNPs) have emerged as a simple and promising route for the modification of surfaces due to the possibility to obtain metallic materials with enhancement of the electrochemical properties (Ariga et al. 2012, Gribova et al. 2012, Iost and Crespilho 2012). For example, gold is generally viewed as a good candidate for hole-injecting contacts due to its work function which is commonly cited as 5.2 eV (Braun et al. 2009). The combination of the transparent ITO electrode and AuNPs can also be a promising strategy for application in spectroelectrochemistry. However, AuNPs absorbs and scatter light efficiently due to the plasmon resonance effects (Srivastava et al. 2005). Herein, we report a methodology to obtain ITO electrodes modified with electrochemically active AuNPs, in which dendritic AuNPs were electrodeposited on ITO electrodes with no significant loss of transparency.

MATERIALS AND METHODS

MATERIALS

The polyelectrolytes PSS, PAMAM dendrimer generation 4 (10% in methanol), tetrachloroauric acid ($HAuCl_4$) (99%), potassium ferricyanide (III) ($K_3Fe(CN)_6$)(99%), potassium ferricyanide (II) trihidrate ($K_4Fe(CN)_6.3H_2O$)(99%) and ITO electrodes (15-25 Ω sq^{-1}) were obtained from Sigma-Aldrich. Gold coated glass with thickness of 100 Å (dimensions of 22mm x 22mm square) was obtained from Sigma-Aldrich. N-dodecanothiol (98%) and ferrocene (98%) were obtained from Sigma Aldrich). Potassium chloride (KCl)(99%) was achieved from Vetec. Sulfuric acid (H_2SO_4) (97-99%) was obtained from Synth. All glasses utilized in reagent preparation were cleaned with $KMnO_4$, H_2SO_4:H_2O_2 (4:1)(v:v) and then, washed with ultrapure water (Milli-Q system, 18 MΩ cm^{-1}) before the preparation of solutions. ITO electrodes were previously cleaned before electrochemical experiments using RCA modified method (Kern 1984).

ELECTROCHEMICAL MEASUREMENTS

Electrochemical experiments were performed in a 30 mL cell containing the working modified electrode of ITO (1.0 cm^2 area), a platinum auxiliary electrode and the reference electrode Ag/$AgCl_{sat}$ using a Potentiostat/Galvanostat μAutolab model AUT70723. Cyclic voltammetry and chronoamperometry was performed using GPES software. All the electrochemical experiments were carried out at room temperature (298 K). EIS measurements were carried out using FRA module software and a theoretical model was obtained using Randles circuit. The Randles circuit consists basically by an electrolyte solution resistance (R_s), a double-layer capacitance at electrode/electrolyte interface (C_{dl}), a resistance of charge transfer through the interface (R_{ct}) and the Warburg impedance (Z_d) (Bard 1980, Vyas et al. 2010). For modelling the system based on multilayers of PSS/PAMAM the adsorption of each bilayer can be associated with introduction of an additional resistance (R_f) to mass transport of redox probes and a contribution of an additional capacitance value (C_f) to modified ITO electrodes. In our EIS studies, this value will be associated with

the global resistance value when ITO electrodes were modified with the polyelectrolytes PSS and PAMAM. Thus, an additional resistance was introducing for modelling the Randles-modified circuit in this case. Moreover, the Randles circuit was used for modelling equivalent-circuit formed for the case of multilayer films of PSS/PAMAM and the different adsorption times for electrodeposited gold nanostructures.

ATOMIC FORCE MICROSCOPY

The atomic force microscopy was carried out with the objective to achieve information of morphology of ITO-PAMAM-$(PSS/PAMAM)_2$-AuNPs modified electrodes. For this purpose, AFM were performed using an AFM/SPM-Microscope-Agilent 5500 in the contact tip mode, resonance frequency of 40Hz, maximum resolution of 75 μm^2 minimum of 50 nm^2, tip step of 0.5 lines per second.

MODIFICATION OF THE ELECTRODES WITH AUNPS

Firstly, the surface of ITO was modified by using layer-by-layer (LbL) methodology by immersing the electrode alternatively in to solutions of anionic (PSS) and cationic (PAMAM) polyelectrolytes and washed in ultrapure water between each successive step. In our case, the dip time of 5 minutes was used to adsorb each polyelectrolyte layer and form ITO-PAMAM-$(PSS/PAMAM)_2$ modified electrodes. After each adsorption step the substrate/film was rinsed and dried with N_2. In this study we used this configuration in order to realize the adsorption of chloroaurate ions ($AuCl_4^-$) and further the formation of gold nanostructures by changing the dipping time of ITO in to the precursor solution of $HAuCl_4$ 1.0 mmol L^{-1}. The reduced gold form (Au^{3+} to Au^0) was carried out by applying a potential of 1.2V (vs. $Ag/AgCl_{sat}$) by chronoamperometry obtaining the ITO-PAMAM-$(PSS/PAMAM)_2$-AuNPs modified electrodes. Further, the electrochemical stability of ITO-PAMAM-$(PSS/PAMAM)_2$-AuNPs electrodes was verified by cyclic voltammetry. For this purpose, cyclic voltammetry and EIS measurements were perform using the same electrode at each experiment.

CONTACT ANGLE MEASUREMENTS

Highly hydrophobic surfaces were achieved by adsorbing n-octadodecanethiol on to ITO-PAMAM-$(PSS/PAMAM)_2$-AuNPs electrodes. For this purpose, we have previously dip the modified electrode in to n-dodecanothiol in chloroform ($CHCl_3$) solution in order to study of wetting properties of the electrodes prepared previously. The final concentration in n-dodecanothiol in CCl_4 was 20%. The previous prepared ITO-PAMAM-$(PSS/PAMAM)_2$ and ITO-PAMAM-$(PSS/PAMAM)_2$ electrodes modified with electrodeposited gold with adsorption times of 5, 10, 30 and 120 minutes (ITO-PAMAM-$(PSS/PAMAM)_2$-AuNPs) were immersed for 5 hours in n-dodecanothiol solution. The contact angle measurements were carry out in KSV CAM 200 goniometer equipment.

RESULTS

DEPOSITION OF AuNPs ON TO ITO SURFACE

The deposition of AuNPs on to ITO surface using electrochemistry can be used to control the growth of metallic nanoparticles with well-defined shape and morphology (Bui et al. 2009). It´s well known that some metallic nanoparticle shows high absorption and scattering in the visible region of the spectrum, as reported in several studies (Bolzan et al. 2005, Tian et al. 2006, Zhang et al. 2004). Firstly, ITO electrode was modified with polyelectrolyte multilayers (PEM) and then the modified electrodes with polyelectrolytes was used to adsorb $AuCl_4^-$ ions by immersion of the electrode in $HAuCl_4$ precursor aqueous solution (1.0 mmol L^{-1}). The PEM consisted in polyamidoamine dendrimer generation 4 (PAMAM-G4) and poly(sodium styrene sulfonate) (PSS) self-assembled onto ITO

by layer-by-layer technique. The self-assembly of 2-bilayer of PSS and PAMAM on ITO (ITO-PAMAM-(PSS/PAMAM)$_2$) provided the fine control of the amount of $AuCl_4^-$ adsorbed onto ITO-modified electrode. The study was carried out for four different adsorption times of $AuCl_4^-$ ions on to ITO-PAMAM-(PSS/PAMAM)$_2$ (5, 10, 30 and 120 minutes). After dipping of ITO-PAMAM-(PSS/PAMAM)$_2$ in different times $AuCl_4^-$ ions were electrochemically reduced to Au^0 electrochemically by using chronoamperometry. Figure 1 shows the schematic representation of each step of fabrication of ITO-PAMAM-(PSS/PAMAM)$_2$ electrodes with Au^{3+} reduced to Au^0 leading to the formation of dendritic structured nanoparticles.

Figure 2a shows the chronoamperometry curves obtained for different adsorption times, as can be observed by the increasing of faradaic current density associated with the quantity of Au^0 deposited on to the electrode surface. Cyclic voltammograms obtained for each electrode shows the increase of the current density upon the increase of electrodeposited gold (Figure 2b). The increase in current peaks at 1.20V (related to Au oxides) is proportional with the amount of metal/metal oxide Au (Qian and Yang 2006). Figure 2c sows the amount of Au (mol cm^{-2}) deposited onto ITO-PAMAM-(PSS/PAMAM)$_2$ using different times of $AuCl_4^-$ adsorption (5, 10, 30 and 120 minutes). Based on chronoamperometry, the amount of Au atoms electrodeposited for each time was estimated as $4.9x10^{-5}$, $5.0x10^{-5}$, $7.2x10^{-5}$ and $8.3x10^{-5}$ mol cm^{-2} for 5, 10, 30 and 120 minutes, respectively. This result corroborates with the X-ray diffraction pattern for ITO-PAMAM-(PSS/PAMAM)$_2$-AuNPs (Figure 2d), where just for indium-tin oxide are observed peaks with high intensity, at $2\theta = 30.1°$, $2\theta = 35.4°$ and $2\theta = 51.3°$ corresponding to <400> and <222> orientations (Jung and Lee 2003). The diffraction pattern with low intensity peaks is attributed for electrodeposited Au crystals, at $2\theta = 39.0°$ and $2\theta = 45.3°$ (<111> and <200> crystal faces)(Lee et al. 2007).

The evaluation of the electron transfer at electrode/electrolyte interface was carried out by EIS and cyclic voltammetry using $[Fe(CN)_6]^{4-}$/$[Fe(CN)_6]^{3-}$ 5 mmol L^{-1} in KCl 0.1 mol L^{-1} as redox probes. At first, ITO electrodes before and after the adsorption of the polyelectrolytes PSS and PAMAM were evaluated. Figure 3a shows the Nyquist plots for ITO-(PSS), ITO-(PAMAM), ITO-PAMAM-(PSS/PAMAM) and ITO-PAMAM-(PSS/PAMAM)$_2$. It is worth mentioning that we are considering here the adsorption of the first PSS layer on to ITO. As expected, ITO-(PSS) showed no significantly change in the R_{ct} values due to the nature of net negative residual charge on the surface of the electrode. The growth of films could be expected when the first layer of cationic polyelectrolyte PAMAM was adsorbed on ITO electrode. The peripheral amino groups of PAMAM are protonated (NH_3^+) at pH 6.3 which can be responsible for the increase in the current densities for $[Fe(CN)_6]^{4-}$/$[Fe(CN)_6]^{3-}$ owing to the difference of positive residual charge on to the surface of the electrode. For the first coating of PAMAM layer the resistance was 14.3 Ω cm^2, with R_{ct} values increasing progressively with the adsorption of the subsequent bilayers up to around 35 Ω cm^2 for ITO-PAMAM-(PSS/PAMAM)$_2$. It is interesting to note that for the adsorption of the subsequent bilayers on to the electrode ITO-PAMAM-(PSS/PAMAM the R_{ct} values increased up to 20.8 Ω cm^2. We assume that this effect is due to PAMAM do not overcompensate the residual negative charge from the ITO-(PSS), as also a possible interfacial overlap of polyelectrolyte layers (Decher 1997). In addition, the adsorption of the second bilayer (ITO-PAMAM-(PSS/PAMAM)$_2$) showed an increase of the value of R_{ct} closer to the value of bare ITO, possibly because of the blocking effect for mass transport of the redox species in solution (Sun et al. 2007, Zhang et al. 2005). We also evaluated the EIS

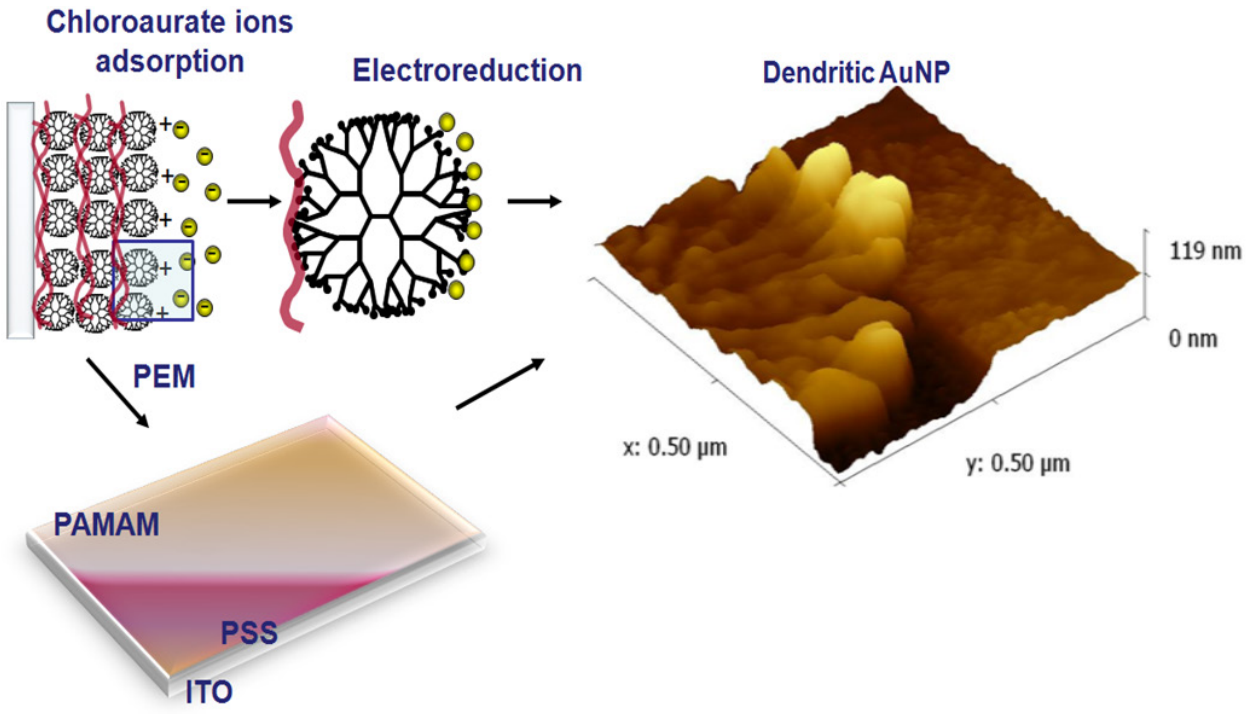

Figure 1 - Schematic representation of each step of fabrication of ITO-PAMAM-$(PSS/PAMAM)_2$ electrodes with adsorption of $AuCl_4^-$ ions. The AFM images show the formation of the dendritic AuNP after electrodeposition (ITO-PAMAM-$(PSS/PAMAM)_2$-AuNPs electrode) by chronoamperometry.

spectrum after the electrodeposition of gold at the surface of the ITO-modified electrodes. Figure 3b shows the Nyquist plots obtained for ITO-PAMAM-$(PSS/PAMAM)_2$-AuNPs electrodes. The EIS results show the increase in the R_{ct} values with the increase in electrodeposited gold on ITO-modified surface (Siqueira et al. 2007). Some studies reports the increase of charge transfer process when AuNPs are synthesized within thin nanostructured films when adsorbed on to the surface of the electrode (Shein et al. 2009, Sze 1981). Shein and co-workers (Hwang and Chen 2001) reported the use of self-assembly monolayers (SAMs) linked to gold nanoparticles with different lengths at which there was an increase in the resistance of charge transfer upon the presence of $[Fe(CN)_6]^{4-}/[Fe(CN)_6]^{3-}$ in solution. This shows the importance of the detailed study of the electrode modification surfaces with nanomaterials with enhanced electrochemical properties with a linear increase in the electron-transfer dependence with the length of SAMs. However, it is important to note that the impedance measurements were conduct with a non-charged macromolecule groups self-assembled on gold electrodes, different of the polyelectrolytes PSS and PAMAM used in here for the preparation of the ITO-modified surface for the growth study of electrodeposited gold. Moreover, the presence of the charged chemical groups reflects directly in the R_{ct} values as observed in Figure 3 (Al-Ibrahim et al. 2005, Liu et al. 1999) and can be clearly observe with variation in adsorption time of $AuCl_4^-$ ions.

Cyclic voltammetry experiments for $[Fe(CN)_6]^{4-}/[Fe(CN)_6]^{3-}$ 5 mmol L^{-1} were also carried out in KCl 0.1 mol L^{-1} for ITO and ITO-PAMAM-$(PSS/PAMAM)_2$-AuNPs electrodes. The two well-defined redox process at 0.32V and 0.20V are attributed to $[Fe(CN)_6]^{4-}$ and $[Fe(CN)_6]^{3-}$, respectively (see the Supplementary Material - Figure S1). First, we have shown the

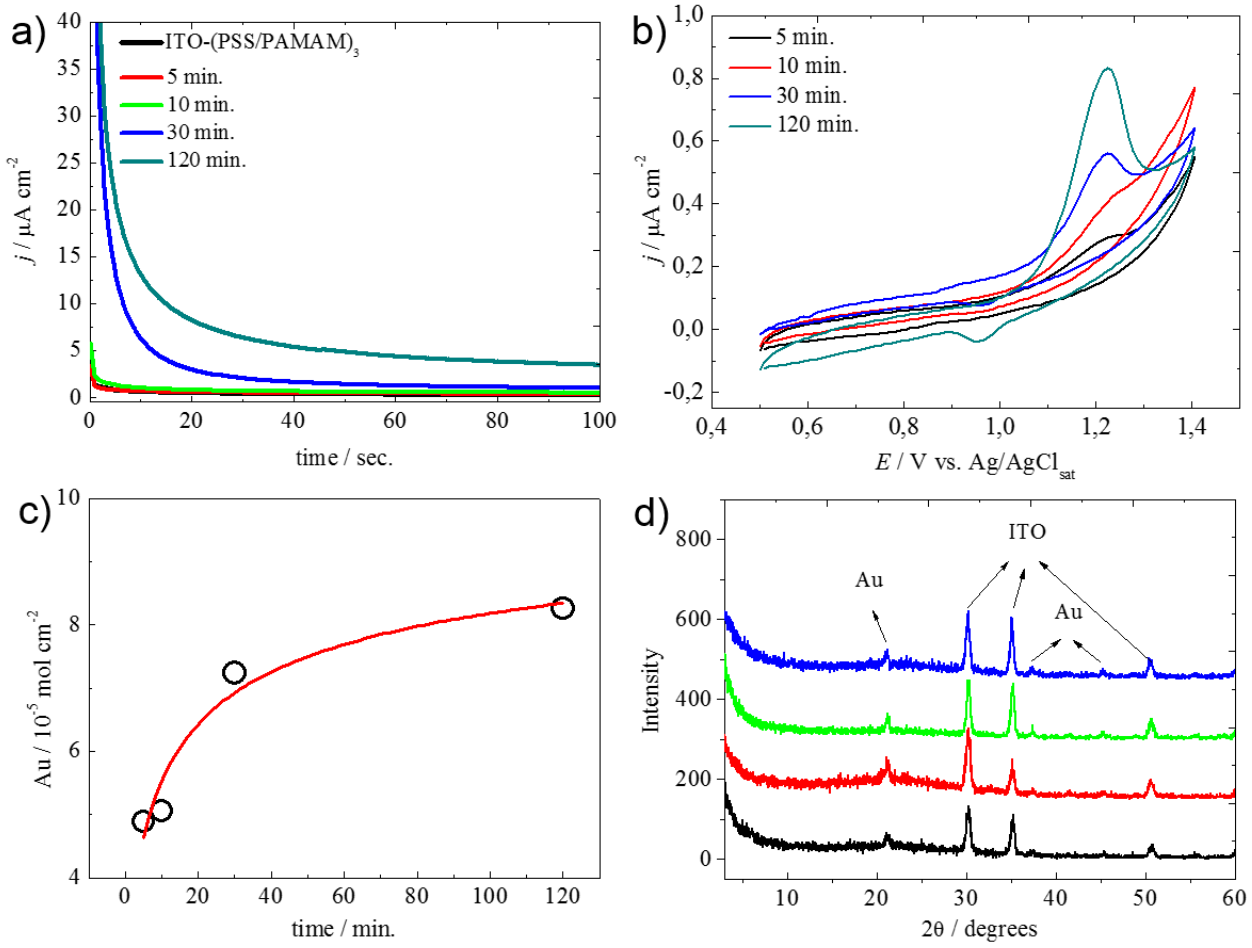

Figure 2 - AuNPs deposition on ITO-PAMAM-$(PSS/PAMAM)_2$ electrodes. For all plots, the color represents: ITO-PAMAM-$(PSS/PAMAM)_2$ (black) and ITO-PAMAM-$(PSS/PAMAM)_2$ electrodes exposed to different times of $AuCl_4^-$ adsorption (5 (red), 10 (green), 30 (blue) and 120 minutes (dark cyan)). Supporting electrolyte: H_2SO_4 0.1 mol L^{-1}. T 25° C. **a)** Chronoamperometric curves (applied potential: 1.2V (vs. $Ag/AgCl_{sat}$). The black curve is superimposed with the red curve. **b)** Cyclic voltammetry after AuNPs deposition. **c)** Amount of Au deposited onto ITO-PAMAM-$(PSS/PAMAM)_2$ using different times of $AuCl_4^-$ adsorption (5, 10, 30 and 120 minutes). **d)** DRX pattern obtained for the ITO-PAMAM-$(PSS/PAMAM)_2$-AuNPs electrodes exposed to different times of $AuCl_4^-$ adsorption (5 (red), 10 (green), 30 (blue) and 120 minutes (dark cyan)).

voltammetric behaviour of ITO and ITO-modified with the self-assembled electrolytes with the redox pair $[Fe(CN)_6]^{4-}/[Fe(CN)_6]^{3-}$. The adsorption of polyelectrolytes PSS, PAMAM and PAMAM-(PSS/PAMAM) upon to bilayers showed an increase in charge-transfer resistance without significant blocking of the surface for the diffusion of the redox species (Figure S1b). The cyclic voltammetry experiments shows an increase in the current densities when the ITO are modified with electrodeposited gold (Figure S1a), as expected due to an increase in the surface area of the electrode by the presence of electrodeposited gold nanostructures. After the adsorption of the first PAMAM layer on ITO, an increase of the current density is observed due to the positive charge of the polyelectrolyte and decreases subsequently with the adsorption of the PSS and PAMAM layers, which acts progressively as a barrier for the diffusion of the $[Fe(CN)_6]^{4-}/[Fe(CN)_6]^{3-}$ species. For this purpose, the experiments were carry out using the same ITO electrode owing to the acquisition

of voltammetric information with subsequent steps of modification with the polyelectrolytes or with the electrodeposited gold nanostructures, as can be observe by the relative small change in the current densities upon the adsorption of the polyelectrolytes. Similar results were obtained for the electrodeposited gold on to ITO electrodes (see Figure S1a). The estimated value for the apparent diffusion coefficient (D_{app}) for $[Fe(CN)_6]^{4-}$/$[Fe(CN)_6]^{3-}$ was estimated as $1x10^{-6}$ cm^2 s^{-1} when ITO and ITO-PAMAM-(PSS/PAMAM)$_2$-AuNPs electrodes were used. The latter is an indication of not only that the surface are not blocked by the particles but also the charge-transport of an external probe redox pair $[Fe(CN)_6]^{4-}$/$[Fe(CN)_6]^{3-}$ from the solution to the electrode surface still occurs efficiently.

WORK FUNCTION FOR ITO MODIFIED ELECTRODE

The determination of the work function (Φ) for ITO modified electrodes is an important factor for practical applications. In a first approach, cyclic voltammetry is commonly used to estimate oxidation potential for HOMO (E_{HOMO}) and LUMO (E_{LUMO}) of polymer modified electrodes (Hwang and Chen 2001). Herein, we have estimate Φ for ITO and ITO modified electrodes with electrodeposited gold by linear sweep voltammetry. For this purpose, we used ferrocene (Fc) adsorbed onto ITO-PAMAM-(PSS/PAMAM)$_2$ and ITO-PAMAM-(PSS/PAMAM)$_2$-AuNPs as an external probe in H_2SO_4 0.1 mol L^{-1} as supporting electrolyte. For ITO electrodes, 100 μL of Fc 5 mmol L^{-1} in ethanol was drop on to the surface and dry under vacuum for 10 minutes before the electrochemical experiments, and ITO-PAMAM-(PSS/PAMAM)$_2$-AuNPs electrodes were dip in of Fc 5 mmol L^{-1} in ethanol for 1 hour before the electrochemistry experiments in order to maintain Fc species adsorbed onto electrodeposited gold. The onset for oxidation potential (E_{ox}) of gold oxides and the onset of oxidation potential for Fc adsorbed species were used in order to estimate Φ for ITO and ITO-PAMAM-(PSS/PAMAM)$_2$ with AuNPs (equation 1)(Liu et al. 1999).

$$\phi=\left[E^{ox}_{onset}\left(\text{vs. Ag/AgCl}\right)-E^{ox}_{onset}\left(Fc/Fc^{+}\text{vs. Ag/AgCl}\right)+4.8)\right]\text{eV} \quad (1)$$

where 4.8 eV is related to the energy work function for Fc at vacuum (Al-Ibrahim et al. 2005). Figure 4a shows the cyclic voltammetry at 50 mV s^{-1} for Fc species dropped (50μL of Fc in ethanol 5 mmol L^{-1}) at ITO electrode and dried at vacuum in absence of heating. It was observed two redox process attributed to oxidation and reduction Fc species at about 0.64V and 0.45V (vs. Ag/AgCl), respectively (Gagne et al. 1980).

The onset oxidation potential was 0.40V (Figure 4b). By using equation 1, Φ was 4.4 eV for Fc adsorbed on to ITO electrodes. The same experiment was carried out for electrode configuration ITO-PAMAM-(PSS/PAMAM)$_2$ with AuNPs with 120 minutes of adsorption. Figure 4c and 4d shows the zoom for the linear sweep voltammogram obtained after the immersion of ITO modified with gold nanoparticles at different overpotential range. Figure 4c shows the onset oxidation potential for Fc species adsorbed onto AuNPs at 0.40 V (vs. Ag/AgCl) and Figure 3d shows the onset oxidation potential for gold oxides (Bolzan et al. 2005) at 1.0 V (vs. Ag/AgCl). As previously described for Fc species adsorbed onto ITO electrode, we have estimate Φ for ITO modified electrodes upon modification with AuNPs since the value of the work function of gold nanoparticles can be influence by the underlying substrate covered with organic molecules. For AuNPs with diameter of 10 nm some studies reported a mismatch of the work function with values of 3.6 eV for Si substrates covered with organic molecules (Zhang et al. 2015). In our case, Φ for ITO-PAMAM-(PSS/PAMAM)$_2$ with AuNPs for adsorption of 120 minutes was found to be similar to bulk gold (5.4 eV) (Magnusson et al. 1999, Zhang et al. 2015).

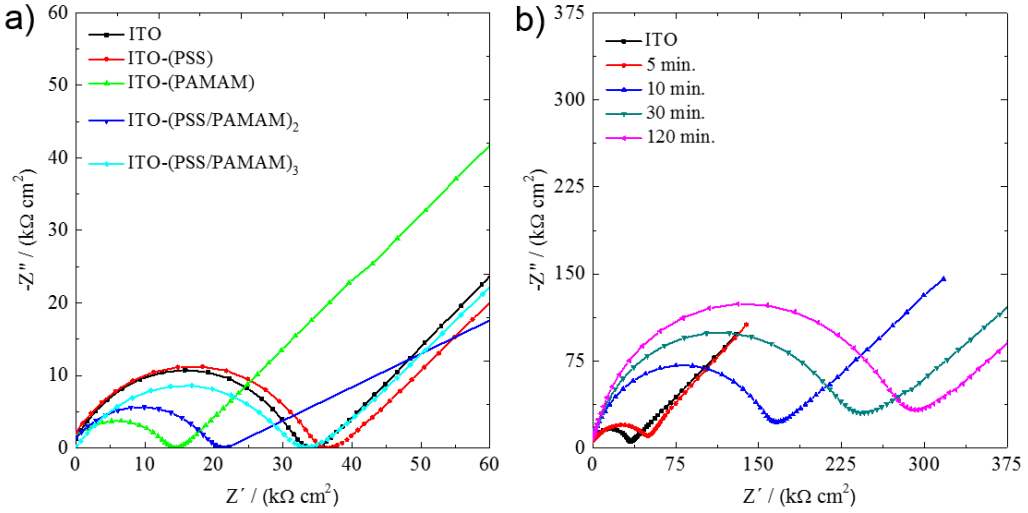

Figure 3 - a) Nyquist impedance spectra for ITO (black) and electrode configurations ITO-(PSS) (red), ITO-(PAMAM) (green), ITO-PAMAM-(PSS/PAMAM)(blue) and ITO-PAMAM-(PSS/PAMAM)$_2$(light blue). **b)** Nyquist impedance spectra for ITO (black) and ITO-PAMAM-(PSS/PAMAM)$_2$ modified gold electrodes with adsorption time of 5 (red),10 (blue),30 (dark green) and 120 minutes (pink) of immersion. Frequency range: 0.1 – 10 kHz. Sinusoidal voltage: 0.1V. Supporting electrolyte: $[Fe(CN)_6]^{4-}/[Fe(CN)_6]^{3-}$ 5 mmol L^{-1} in KCl 0.1 mol L^{-1}. T 25° C. The ITO modified electrodes were immersed in electrolyte solution for 5 minutes before EIS measurements.

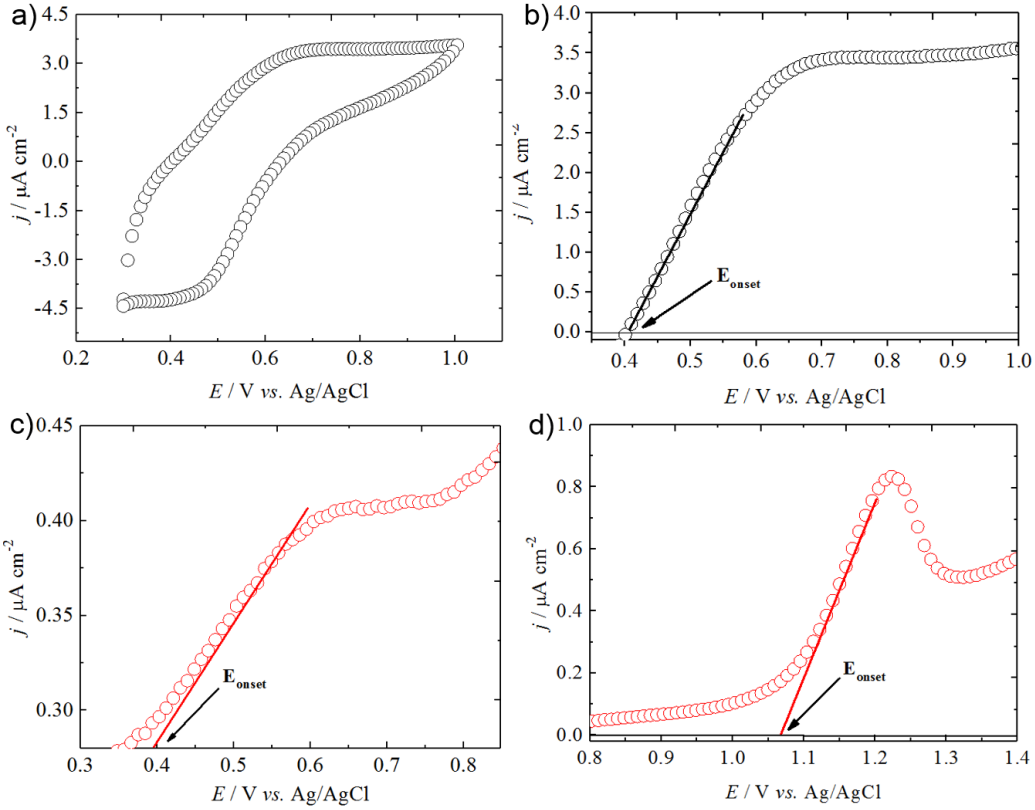

Figure 4 - a) Cyclic voltammogram of Fc species adsorbed onto ITO electrode surface. **b)** Zoom shows E_{onset} oxidation potential for Fc adsorbed species onto ITO electrode. Scan rate: 50 mV s^{-1}. Supporting electrolyte: H_2SO_4 0.1 mol L^{-1}. T 25°C. **c)** Linear sweep voltammogram of Fc species adsorbed onto ITO-PAMAM-(PSS/PAMAM)$_2$ with AuNPs and **d)** linear sweep voltammogram ITO-PAMAM-(PSS/PAMAM)$_2$ with AuNPs for adsorption of 120 minutes. Scan rate: 50 mV s^{-1}. Supporting electrolyte: H_2SO_4 0.1 mol L^{-1}. T 25° C.

MORPHOLOGICAL PROPERTIES OF DENDRITIC AuNPs

The shape and morphology of the dendritic gold particles were investigated by AFM. It was observe the formation of dendritic gold nanostructures on ITO-modified PEM electrodes, as shown in Figure 5a. We emphasize here the formation of gold dendrites in nanoscale size when the adsorption of $AuCl_4^-$ are carry out previously to the chronoamperometric reduction of ITO modified electrodes with polyelectrolytes. The Au atoms distributed on a surface density of $8.3x10^{-5}$ mol cm^{-2} (120 min) leaded to nanoparticles with dendritic forms with radius of 300 nm and thickness of 59 nm, as observed by AFM images (Figure 5b). Figure S2 shows the counting of 100 distances between dendritic structures of electrodeposited AuNPs onto ITO-PAMAM-$(PSS/PAMAM)_2$ electrodes for the adsorption time of 120 minutes versus distance of each dendritic AuNPs structures. The dendritic AuNPs show high homogeneity on ITO surface with distances ranging from 4 to 46 nm between them with selected area of 600 x 20 µm. The determination of the distances between each dendritic gold structure was carry out using the Image J software, image processing data.

OPTICAL AND SURFACE PROPERTIES OF ITO MODIFIED WITH AuNPs

The influence of the AuNP on the optical properties of ITO was also investigate by electronic

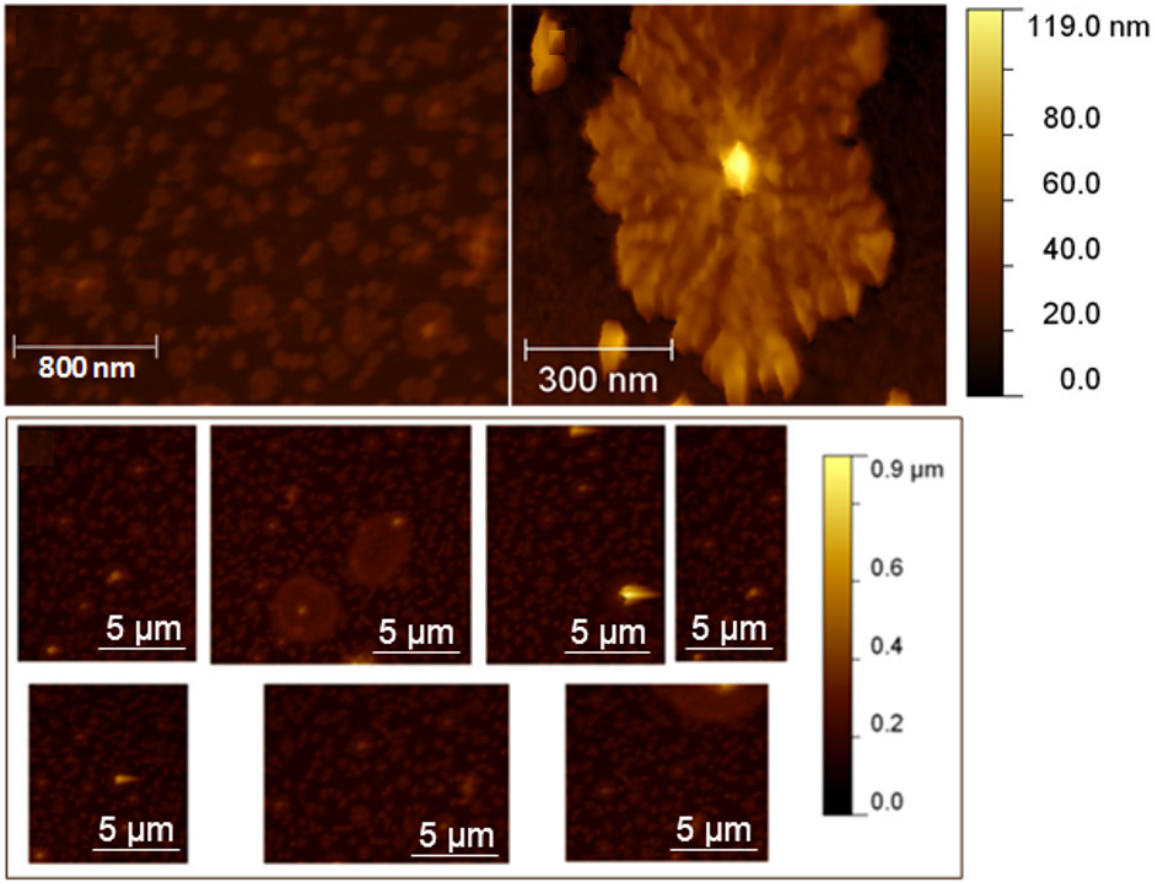

Figure 5 - a) AFM image of ITO-PAMAM-$(PSS/PAMAM)_2$-AuNPs electrodes using the adsorption time of 120 minutes. **b)** Zoom of dendritic AuNP structure. **c)** AFM images of ITO-PAMAM-$(PSS/PAMAM)_3$-AuNPs shows the distribution of dendritic structures over the surface of ITO modified electrode.

spectroscopy in visible region (400 to 800 nm). Figure 6 shows the electronic spectra for ITO and ITO-PAMAM-(PSS/PAMAM)$_2$ modified with electrodeposited gold at 120 minutes. ITO-PAMAM-(PSS/PAMAM)$_2$-AuNPs is an electrode with the gold surface properties and with similar optical properties of ITO. The optical properties of ITO modified electrodes with a high controlled gold coated glass with thickness of 10 nm (dimensions of 22 mm x 22 mm square) was compared with a thicker film of Au deposited over glass substrate. For this case, the sputtering methodology was used for the obtention of a gold film over glass substrate with thickness of 66 nm (thickness data was obtain using Dekta K 150 equipment). Figure 6 shows the transmittance spectrum (%) obtained for baseline (black), for ITO (red), ITO-PAMAM-(PSS/PAMAM)$_2$-AuNPs (pink), glass lamine Au-coated with 10 nm of thickness (blue) and glass lamine Au-coated with 66 nm of thickness (green). Considering the optical properties of the electrodes, the loss of transparency in ITO electrode was about 10% upon electrodeposition of AuNPs. The previous modification of ITO with polyelectrolytes provided the control of gold deposition and the methodology used here was able to achieve ITO electrodes with no significant loss of their original transparency once dendritic AuNPs homogeneously dispersed on ITO. Generally, electrodeposited gold nanostructure shows well-defined broadband peaks at visible region from 500 to 600 nm (Ye et al. 2010). Here, ITO-PAMAM-(PSS/PAMAM)$_2$-AuNPs showed no significant change in the transmittance when compared to ITO electrodes. This result may relate to the shape, size of dendritic gold structures and with the distance between each other, as shown previously in AFM images. Furthermore, the spectrum shows clearly the influence of thickness on transmittance when comparing a less thick gold coated and a denser gold coated deposited onto a glass substrate with the obtained ITO modified with AuNPs. For example, in Figure 6 it is possible to

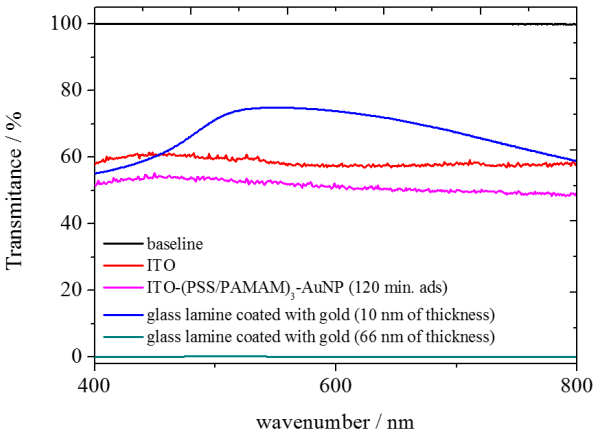

Figure 6 - Electronic spectroscopy at visible range of baseline in air (black), ITO (red), ITO-PAMAM-(PSS/PAMAM)$_2$-AuNPs (pink), glass lamine Au-coated with 10 nm of thickness (blue) and glass lamine Au-coated with 66 nm of thickness (green).

observe that a glass lamine Au-coated with 66 nm of thickness (green spectrum) could not be used in spectroelectrochemistry experiments in absorbance mode since it is not transparent to visible light.

We also show how AuNPs on the surface can be explored as versatile material for possible applications. This includes functionalization or other process that are dependent of gold contact on surface. For instance and beyond electrochemical devices applications, this electrode becomes interesting for use as hydrophobic surfaces (Zhang et al. 2004). In a typical hydrophilic surface the contact angle of water ranges from 0° to 30° (Ye et al. 2010) with the energy of interaction changing with the increase in hydrophobicity due to a low energy of interaction with the surface (Hong et al. 2009, Kwok and Neumann 1999). An increase of the static contact angle of water with the presence of AuNP from 59.9° to 66.4° was firstly observed, as shown in Figure 5. It is well known that the presence of sulfur groups can adsorb onto gold surface and on to gold nanoparticles deposited on to ITO. Table I shows the contact angles measurements obtained and Figure 7a-d show the figures of water droplet onto ITO and ITO modified with AuNPs. As observed in table I,

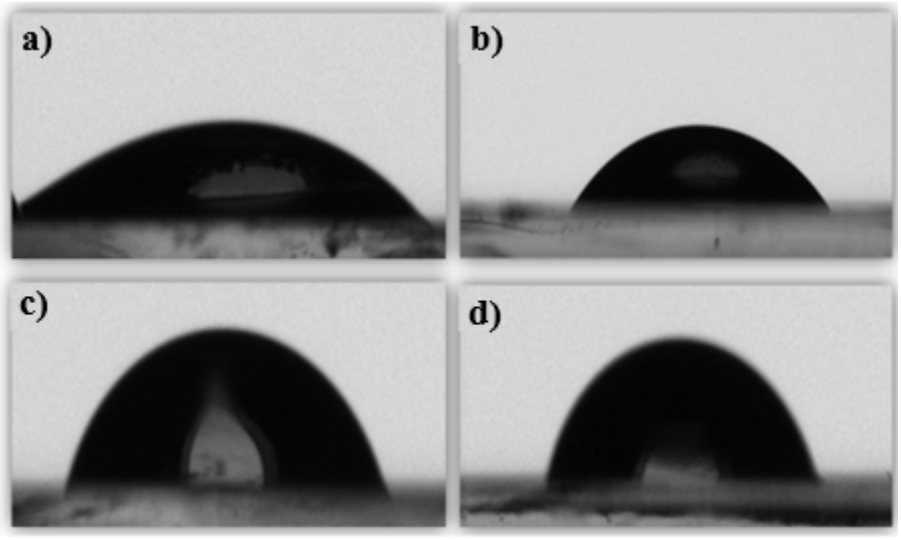

Figure 7 - Contact angle measurements on the surface of ITO modified AuNPs as a function of adsorption time of $AuCl_4^-$. The contact angle for each sample were measured by dropping 2 μL of distilled water onto ITO and ITO modified surfaces before and after the adsorption of n-dodecanothiol. Static contact angle for **a)** ITO-PAMAM-$(PSS/PAMAM)_2$, **b)** ITO-PAMAM-$(PSS/PAMAM)_2$ modified with AuNPs at 5 min, **c)** 30 min and **d)** 120 minutes of adsorption. Immersion time in n-dodecanothiol solution (20%): 5 hours.

TABLE I
Contact angle measurements for ITO-PAMAM-(PSS/PAMAM)2-AuNPs electrodes modified with n-dodecanothiol.

Time (min)	Θ_{left} (°)	Θ_{right} (°)	Θ_{medium} (°)
0	57.9	62.0	59.9
5	58.6	56.7	57.6
30	62.7	60.5	61.7
120	66.5	66.4	66.4

the contact angles increased from 59.9° to 66.4° with the increasing of adsorption time of ions $AuCl_4^-$. The formation of dendritic-like structures can also contribute for the increase in contact angle and for the hydrophobicity (Dutta et al. 2007, Zhang et al. 2004).

CONCLUSIONS

We reported a strategy to obtain ITO electrodes modified with self-assembled polyelectrolytes and active dendritic AuNPs. This is a typical combination of soft and metallic materials that results in electrodes with significant maintenance of optical transparency compared with bare ITO. We showed here the influence of the adsorption of polyelectrolytes and AuNPs on the electrochemistry, morphology and optical properties of ITO-modified electrodes. The transparency of the ITO modified with gold dendrites are significantly preserved at the same time providing electroactive gold sites at electrode surface. We propose that dendritic AuNPs on the ITO surface can also be explored as a versatile material for new applications, such as surface functionalization and hydrophobic surfaces. Additionally, the combination of all these characteristics is promising to produce alternative electrodes to be applied in spectroelectrochemistry studies.

ACKNOWLEDGMENTS

The authors gratefully acknowledge Brazilian agencies including Fundação de Amparo à Pesquisa do Estado de São Paulo (FAPESP, F. N. Crespilho, projects numbers: 2015/16672-3, 2013/14262-

7 and 2013/04663-4); Conselho Nacional de Desenvolvimento Científico e Tecnológico (CNPq, F. N. Crespilho, project numbers: 306106/2013-2 and 478525/2013-3). Rodrigo M. Iost specially acknowledge FAPESP for his master fellowship, process number 2009/12000-0. This study was also supported in part by the Coordenação de Aperfeiçoamento de Pessoal de Nível Superior - Brasil (CAPES) - Finance Code 001.

AUTHOR CONTRIBUTIONS

RMI and MVAM contributed with the experiments and wrote the manuscript. FNC supervised the project and wrote the manuscript.

REFERENCES

AL-IBRAHIM M, ROTH HK, SCHROEDNER M, KONKIN A, ZHOKHAVETS U, GOBSCH G, SCHARFF P AND SENSFUSS S. 2005. The influence of the optoelectronic properties of poly(3-alkylthiophenes) on the device parameters in flexible polymer solar cells. Org Electron 6: 65-77.

ARIGA K, JI QM, HILL JP, BANDO Y AND AONO M. 2012. Forming nanomaterials as layered functional structures toward materials nanoarchitectonics. Npg Asia Mater 4: 1-11.

ARMSTRONG NR, CARTER C, DONLEY C, SIMMONDS A, LEE P, BRUMBACH M, KIPPELEN B, DOMERCQ B AND YOO SY. 2003. Interface modification of ITO thin films: organic photovoltaic cells. Thin Solid Films 445: 342-352.

BARD, AJ AND FAULKNER LR. 1980. Electrochemical Methods: Fundamentals and Applications, New York: J Wiley & Sons, New York, USA, p 864.

BOLZAN AE, IWASITA T AND ARVIA AJ. 2005. Combined voltammetry and in situ infrared spectroscopy of tetramethylthiourea on gold in aqueous acid solutions. Electrochim Acta 51: 1044-1058.

BRAUN S, SALANECK WR AND FAHLMAN M. 2009. Energy-Level Alignment at Organic/Metal and Organic/Organic Interfaces. Adv Mater 21: 1450-1472.

BUI MPN, LEE S, HAN KN, PHAM XH, LI CA, CHOO J AND SEONG GH. 2009. Electrochemical patterning of gold nanoparticles on transparent single-walled carbon nanotube films. Chem Commun 37: 5549-5551.

CHEN Y, ZHANG X, YU P AND MA YW. 2009. Stable dispersions of graphene and highly conducting graphene films: a new approach to creating colloids of graphene monolayers. Chem Commun 30: 4527-4529.

DECHER G. 1997. Fuzzy Nanoassemblies Toward Layered Polymeric Multicomposites. Science 277: 1232-1237.

DOMINGUES SH, SALVATIERRA RV, OLIVEIRA MM AND ZARBIN AJG. 2011. Transparent and conductive thin films of graphene/polyaniline nanocomposites prepared through interfacial polymerization. Chem Commun 47: 2592-2594.

DUTTA P, PAL S, SEEHRA MS, ANAND M AND ROBERTS CB. 2007. Magnetism in dodecanethiol-capped gold nanoparticles: Role of size and capping agent. Appl Phys Lett 90: 213102

GAGNE RR, KOVAL CA AND LISENSKY GC. 1980. Ferrocene as an Internal Standard for Electrochemical Measurements. Inorg Chem 19, 2854-2855.

GRIBOVA V, AUZELY-VELTY R AND PICART C. 2012. Polyelectrolyte Multilayer Assemblies on Materials Surfaces: From Cell Adhesion to Tissue Engineering. Chem Mater 24: 854-869.

HONG SD, HA MY AND BALACHANDAR S. 2009. Static and dynamic contact angles of water droplet on a solid surface using molecular dynamics simulation. J Colloid Interf Sci 339: 187-195.

HWANG SW AND CHEN Y. 2001. Synthesis and electrochemical and optical properties of novel poly(aryl ether)s with isolated carbazole and p-quaterphenyl chromophores. Macromolecules 34: 2981-2986.

IOST RM AND CRESPILHO FN. 2012. Layer-by-layer self-assembly and electrochemistry: Applications in biosensing and bioelectronics. Biosens Bioelectron 31: 1-10.

ITO S, NAZEERUDDIN MK, ZAKEERUDDIN SM, PECHY P, COMTE P, GRATZEL M, MIZUNO T, TANAKA A AND KOYANAGI T. 2009. Study of Dye-Sensitized Solar Cells by Scanning Electron Micrograph Observation and Thickness Optimization of Porous TiO_2 Electrodes. Int J Photoenergy 2009: 1-8.

JUNG YS AND LEE SS. 2003. Development of indium tin oxide film texture during DC magnetron sputtering deposition. J Cryst Growth 259: 343-351.

KERN W. 1984. Semiconductor International, 7: p 94.

KWOK DY AND NEUMANN AW. 1999. Contact angle measurement and contact angle interpretation. Adv Colloid Interfac 81: 167-249.

LEE KY, HWANG J, LEE YW, KIM J AND HAN SW. 2007. One-step synthesis of gold nanoparticles using azacryptand and their applications in SERS and catalysis. J Colloid Interf Sci 316: 476-481.

LI J, HU L, WANG L, ZHOU Y, GRUNER G AND MARKS TJ. 2006. Organic light-emitting diodes having carbon nanotube anodes. Nano Lett 6: 2472-2477.

LIU Y, LIU MS AND JEN AKY. 1999. Synthesis and characterization of a novel and highly efficient light-emitting polymer. Acta Polym 50: 105-108.

MADARIA AR, KUMAR A, ISHIKAWA FN AND ZHOU CW. 2010. Uniform, Highly Conductive, and Patterned Transparent Films of a Percolating Silver Nanowire Network on Rigid and Flexible Substrates Using a Dry Transfer Technique. Nano Res 3: 564-573.

MAGNUSSON MH, DEPPERT K, MALM JO, BOVIN JO AND SAMUELSON L. 1999. Gold nanoparticles: Production, reshaping, and thermal charging. J Nanopart Res 1: 243-251.

QIAN L AND YANG XR. 2006. Polyamidoamine dendrimers-assisted electrodeposition of gold-platinum bimetallic nanoflowers. J Phys Chem B 110: 16672-16678.

RICHARDSON JB AND CARUSO F. 2015. Technology-driven layer-by-layer assembly of nanofilms. Science 348(2491): aaa2491.

SAPP SA, SOTZING GA AND REYNOLDS JR. 1998. High contrast ratio and fast-switching dual polymer electrochromic devices. Chem Mater 10: 2101-2108.

SHEIN JB, LAI LMH, EGGERS PK, PADDON-ROW MN AND GOODING JJ. 2009. Formation of Efficient Electron Transfer Pathways by Adsorbing Gold Nanoparticles to Self-Assembled Monolayer Modified Electrodes. Langmuir 25: 11121-11128.

SIQUEIRA JR, CRESPILHO FN, ZUCOLOTTO V AND OLIVEIRA ON. 2007. Bifunctional electroactive nanostructured membranes. Electrochem Commun 9: 2676-2680.

SRIVASTAVA S, FRANKAMP BL AND ROTELLO VM. 2005. Controlled plasmon resonance of gold nanoparticles self-assembled with PAMAM dendrimers. Chem Mater 17: 487-490.

SUN YY, BAI Y, YANG WW AND SUN CQ. 2007. Controlled multilayer films of sulfonate-capped gold nanoparticles/thionine used for construction of a reagentless bienzymatic glucose biosensor. Electrochim Acta 52: 7352-7361.

SZE SM. 1981. Physics of Semiconductor Devices, 2nd ed., New York: J Wiley & Sons, New York, USA, p. 868.

TIAN Y, LIU HQ, ZHAO GH AND TATSUMA T. 2006. Shape-controlled electrodeposition of gold nanostructures. J Phys Chem B 110: 23478-23481.

VYAS RN, LI KY AND WANG B. 2010. Modifying Randles Circuit for Analysis of Polyoxometalate Layer-by-Layer Films. J Phys Chem B 114: 15818-15824.

YAN H, LEE P, ARMSTRONG NR, GRAHAM A, EVMENENKO GA, DUTTA P AND MARKS TJ. 2005. High-performance hole-transport layers for polymer light-emitting diodes. Implementation of organosiloxane cross-linking chemistry in polymeric electroluminescent devices. J Am Chem Soc 127: 3172-3183.

YE WC, YAN JF, YE QA AND ZHOU F. 2010. Template-Free and Direct Electrochemical Deposition of Hierarchical Dendritic Gold Microstructures: Growth and Their Multiple Applications. J Phys Chem C 114: 15617-15624.

ZHANG JD, KAMBAYASHI M AND OYAMA M. 2005. Seed mediated growth of gold nanoparticles on indium tin oxide electrodes: Electrochemical characterization and evaluation. Electroanal 17: 408-416.

ZHANG X, SHI F, YU X, LIU H, FU Y, WANG ZQ, JIANG L AND LI XY. 2004. Polyelectrolyte multilayer as matrix for electrochemical deposition of gold clusters: toward super-hydrophobic surface. J Am Chem Soc 126: 3064-3065.

ZHANG Y, PLUCHERY O, CAILLARD L, LAMIC-HUMBLOT AF, CASALE S, CHABAL YJ AND SALMERON M. 2015. Sensing the charge state of single gold nanoparticles via work function measurements. Nano Lett 15: 51-55.

ZHAO L, ZHAO L, XU YX, QIU TF, ZHI LJ AND SHI GQ 2009. Polyaniline electrochromic devices with transparent graphene electrodes. Electrochim Acta 55: 491-497.

SUPPLEMENTARY INFORMATION

Figure S1 - a) Cyclic voltammetry obtained for ITO (black) and ITO-PAMAM-$(PSS/PAMAM)_2$ modified electrodes with different times of $AuCl_4^-$ adsorption (5 (red), 30 (green) and 120 minutes (blue). **b)** Cyclic voltammetry for ITO (black), ITO-(PAMAM) (red), ITO-PAMAM-(PSS/PAMAM) (green) and ITO-PAMAM-$(PSS/PAMAM)_2$ (blue). Supporting electrolyte: H_2SO_4 0.1 mol L^{-1}. T 25° C.

Figure S2 - Distance distribution histogram of the counting number of 100 dendritic AuNPs distances vs. distance between each dendritic AuNPs structures evaluated by the AFM image of figure 5a. Selected area: 600 x 20 μm (Image J software, image processing and analysis).